AEROSPACE REPORT NO.
ATR-78(8114)-1

MASTER

Impedance Measurements on Sealed Lead-Acid Cells

Prepared by M. R. MARTINELLI and A. H. ZIMMERMAN
Chemistry and Physics Laboratory

10 May 1978

Prepared for VICE PRESIDENT AND GENERAL MANAGER
THE IVAN A. GETTING LABORATORIES

The Ivan A. Getting Laboratories
THE AEROSPACE CORPORATION

DISCLAIMER

THE IVAN A. GETTING LABORATORIES

The Laboratory Operations of The Aerospace Corporation is conducting experimental and theoretical investigations necessary for the evaluation and application of scientific advances to new military concepts and systems. Versatility and flexibility have been developed to a high degree by the laboratory personnel in dealing with the many problems encountered in the nation's rapidly developing space and missile systems. Expertise in the latest scientific developments is vital to the accomplishment of tasks related to these problems. The laboratories that contribute to this research are:

Aerophysics Laboratory: Launch and reentry aerodynamics, heat transfer, reentry physics, chemical kinetics, structural mechanics, flight dynamics, atmospheric pollution, and high-power gas lasers.

Chemistry and Physics Laboratory: Atmospheric reactions and atmospheric optics, chemical reactions in polluted atmospheres, chemical reactions of excited species in rocket plumes, chemical thermodynamics, plasma and laser-induced reactions, laser chemistry, propulsion chemistry, space vacuum and radiation effects on materials, lubrication and surface phenomena, photosensitive materials and sensors, high precision laser ranging, and the application of physics and chemistry to problems of law enforcement and biomedicine.

Electronics Research Laboratory: Electromagnetic theory, devices, and propagation phenomena, including plasma electromagnetics; quantum electronics, lasers, and electro-optics; communication sciences, applied electronics, semiconducting, superconducting, and crystal device physics, optical and acoustical imaging; atmospheric pollution; millimeter wave and far-infrared technology.

Materials Sciences Laboratory: Development of new materials; metal matrix composites and new forms of carbon; test and evaluation of graphite and ceramics in reentry; spacecraft materials and electronic components in nuclear weapons environment; application of fracture mechanics to stress corrosion and fatigue-induced fractures in structural metals.

Space Sciences Laboratory: Atmospheric and ionospheric physics, radiation from the atmosphere, density and composition of the atmosphere, aurorae and airglow; magnetospheric physics, cosmic rays, generation and propagation of plasma waves in the magnetosphere; solar physics, studies of solar magnetic fields; space astronomy, x-ray astronomy; the effects of nuclear explosions, magnetic storms, and solar activity on the earth's atmosphere, ionosphere, and magnetosphere; the effects of optical, electromagnetic, and particulate radiations in space on space systems.

THE AEROSPACE CORPORATION
El Segundo, California

• • •

Aerospace Report No.
ATR-78(8114)-1

IMPEDANCE MEASUREMENTS ON SEALED LEAD-ACID CELLS

Prepared by

M. R. Martinelli and A. H. Zimmerman
Chemistry and Physics Laboratory

10 May 1978

The Ivan A. Getting Laboratories
THE AEROSPACE CORPORATION
El Segundo, Calif. 90245

Prepared for

VICE PRESIDENT AND GENERAL MANAGER
THE IVAN A. GETTING LABORATORIES

THIS PAGE

WAS INTENTIONALLY

LEFT BLANK

Report No.
ATR-78(8114)-1

IMPEDANCE MEASUREMENTS ON SEALED LEAD-ACID CELLS

Prepared

M. R. Martinelli

A. H. Zimmerman

Approved

S. Feuerstein, Head
Interfacial Sciences Department

S. Siegel, Director
Chemistry and Physics Laboratory

THIS PAGE
WAS INTENTIONALLY
LEFT BLANK

ABSTRACT

The impedance of sealed 2.5 ampere hour lead-acid cells has been measured as a function of state of charge at frequencies of 10 Hz to 500 KHz. The impedance of a small lead-acid wet cell employing flat plate electrodes has also been measured over this frequency range. Comparisons between the results for these two cell types indicate that impedances are sensitive to chemical and physical changes which accompany cell discharge. A model is proposed which relates inductive behavior for porous electrodes to the electrode structure. Double layer capacities are estimated for the two types of lead-acid cells.

THIS PAGE
WAS INTENTIONALLY
LEFT BLANK

CONTENTS

FIGURES

Impedance Measurements on Sealed Pb/H_2SO_4 Cells

At present the Pb/H_2SO_4 galvanic cell is one of the most commonly employed cells in battery systems. The performance characteristics of Pb/H_2SO_4 cells depend not only on the chemical and electrochemical reactions which occur during storage, charge, and discharge; but are also critically dependent on the physical configuration and morphology of the active materials as well as the ease with which mass transport can occur within the cell. The interplay of these effects combined with the fact that the properties and structures of the electrodes are continuously being modified by the passage of current, make it difficult to apply standard methods of electrochemical kinetics to the characterization of battery cell processes.

Frequency dependent impedance measurements have seen limited application in the past to studying the electrochemical and physical properties of battery cells. Several previous studies have been directed toward LeClanche type cells[1] and nickel cadmium cells[2]. Recently the impedances of standard Pb/H_2SO_4 wet cells have been reported[3] by Keddam, Stoynov, and Takenouti. While quantitative interpretation of frequency dependent impedances are sometimes difficult, they usually can provide qualitative information which is useful for characterizing the chemical and physical changes which accompany the charge or discharge of a battery cell.

An important complication which must be considered when measuring the impedance of battery cells is that during charge and discharge the cell is never in a steady state. For this reason these measurements

must be made in a time interval which is short enough so that, during the course of the measurement, cell properties remain essentially unchanged. This interval will depend on the rates at which cell properties change, and thereby on the current flowing through the cell as well as the cell state of charge. With appropriately short measurement times the cell impedance can be determined during charge or discharge at near steady state conditions.

During a recent investigation[4] of the relationship between the impedance properties of sealed Pb/H_2SO_4 cells and their state of charge, the change in the phase angle between an applied alternating voltage and the current response was found to correlate with state of charge. The phase angle became increasingly less capacitive with cell discharge, the magnitude of the effect increasing as the frequency was decreased. One purpose of this study is to characterize the cell changes which cause the phase angle, or cell impedance, to change in this manner. Impedance measurements are reported for commercially available sealed Pb/H_2SO_4 cells as well as for small flooded cells incorporating flat plate electrodes. These measurements should allow the impedance of cells having porous, electrolyte starved electrodes to be compared with that of cells having flat, electrolyte-flooded electrodes.

Experimental

The sealed Pb/H_2SO_4 cells studied here were 2.5 ampere hour D size cells produced by Gates Energy Products. These cells have the active materials pasted onto lead grids, which are spirally wound so as to fit into a cylindrical can. They contain only enough electrolyte to wet

the separator material. The cells were brought to full charge using a Gates Energy Products 6 volt hybrid charger for a minimum charge time of 24 hours. The charged cells were allowed to stand overnight on open circuit to stabilize, after which the cell potentials were typically 2.175 to 2.180 volts. All experiments were performed at a temperature of $23 \pm 2^{o}C$.

For sufficiently low discharge currents the cell voltage did not change by more than 0.5 mV over the course of an impedance measurement (about 12 minutes). Measurements were made at a number of states of charge at discharge rates of 1, 20, and 50 mA. The cells were allowed to stabilize for at least 30 minutes at each discharge current prior to impedance measurements. Near total discharge, measurements could only be made at the 1 mA discharge rate, since the higher rates led to unacceptably rapid changes in cell voltage. The zero state of charge is defined to be that obtained when the cell potential reaches 1.500 volts with a 50 mA (C/50) discharge rate.

The electrodes for the Pb/H_2SO_4 wet cell were circular lead plates 3.8 cm in diameter and 1 mm thick. The electrodes were separated by a 4.7 cm diameter, 1.1 mm thick glass fiber separator. The electrodes had lead wires (Pb) spot-welded to them and the electrode/separator assembly was held in a plexiglass holder. The electrolyte consisted of H_2SO_4 having a density of 1.22, which was made by diluting reagent H_2SO_4 (density 1.84) with deionized water.

Impedance measurements for the wet cell were made at specific cell voltages ranging from 1.50 to 2.15 volts. The specific cell voltages were maintained by a potentiostat during the measurements.

Measurements were made 30 minutes after stabilizing the cell voltage at each given value.

Impedance measurements were made by applying low amplitude sinusoidal voltages to the cell using the apparatus shown in Figure 1. The resistance R_L is adjusted to give the desired discharge current through the cell. A reference resistor consisting of about 1 cm of nichrome wire and having a resistance of 0.0118Ω was used in all measurements. This resistor was calibrated to $\pm$ 2% in the circuit of Figure 1 as well as separately using a B224 Wayne-Kerr bridge. The amplitude of the sinusoidal signal applied to the cell was 2 mV. The voltage across the reference resistor was input to channel A of an HP-3575A gain-phase meter, while the voltage across both the cell and the reference resistor were input to channel B. The relative AC voltage across the cell is monitored as the logarithmic difference X, between channels A and B. This amplitude in dBV as well as the phase difference θ between A and B is displayed on a digital voltmeter. These quantities are combined with the value of the reference resistor R_o, to give the real and complex components of the cell impedance.

$$\text{Re}(Z) = R_o [\cos\theta \exp(0.1151\,X) - 1]$$

$$\text{Im}(Z) = R_o \sin\theta \exp(0.1151\,X)$$

These components are plotted in the complex plane $Z = R - jG$ as functions of frequency. The apparatus which was used enables impedances down to less than 1 mΩ to be accurately measured over the frequency range of 10 Hz to 500 kHz.

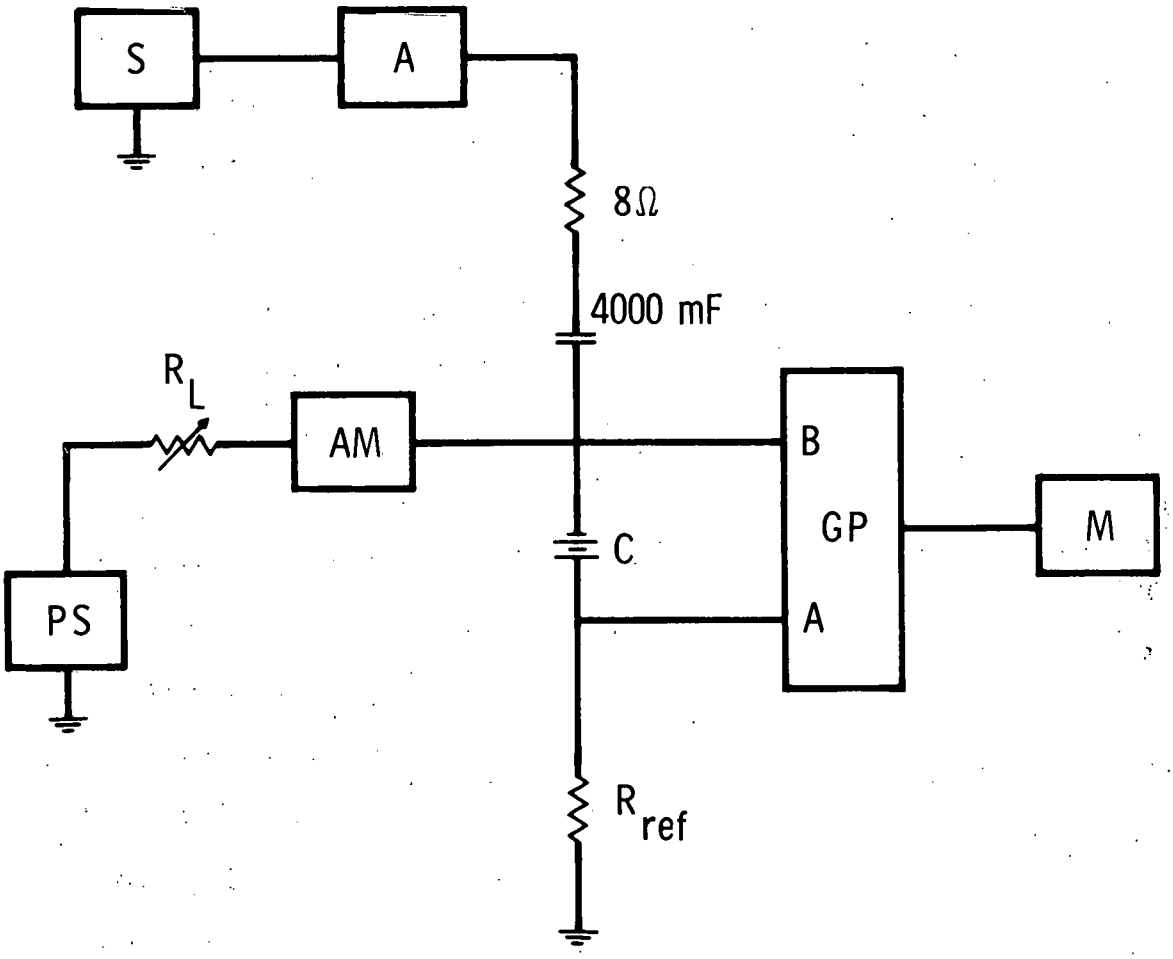

Fig. 1. Instrumentation Used to Measure Impedances of Pb/H_2SO_4 Cells. S is the sine wave generator, A the broadband amplifier, C the battery cell, R_{ref} the reference resistor, GP the gain-phase meter, M a digital voltmeter, AM is a milliammeter, R_L a variable load resistor, and PS thc bias power supply. The 8Ω resistor is the amplifier load resistor and the 4000 μF capacitor a blocking capacitor.

Results

A. Sealed Pb/H_2SO_4 Cells.

The results of impedance measurements as a function of frequency for a sealed Pb/H_2SO_4 cell at states of charge ranging from fully charged to fully discharged are presented in Figures 2 - 5 for discharge rates of 1 mA. Measurements performed on other cells showed small cell to cell variations in the impedance at each state of charge, however the overall trends in impedance as the cells were discharged were the same as those shown in Figures 2 - 5. The impedances presented in these figures are between the positive and negative terminals of the cells, and will therefore consist of the series impedance of both electrodes and the intervening electrolyte.

In all cases cell impedances tend to be capacitive at low frequencies and inductive at high frequencies, with the degree of inductive character diminishing with cell discharge. Small changes in impedance were observed as the discharge rate was varied at each state of charge. The higher discharge rates tended both to decrease the size of the capacitive arc observed at frequencies less than 500 Hz, and to slightly increase the size of the small capacitive arc at about 3 KHz.

One of the more prominent features in the impedance of Pb/H_2SO_4 cells is a large high frequency inductive arc which schematically resembles an inductor shunted by a parallel resistor. This inductance is independent of discharge current and if the cell is more than about 20% charged it is essentially independent of state of charge. This type of self inductance has been previously observed for battery cells[3,5-7] and may qualitatively be attributed to the geometrical arrangement of electrodes and conductors

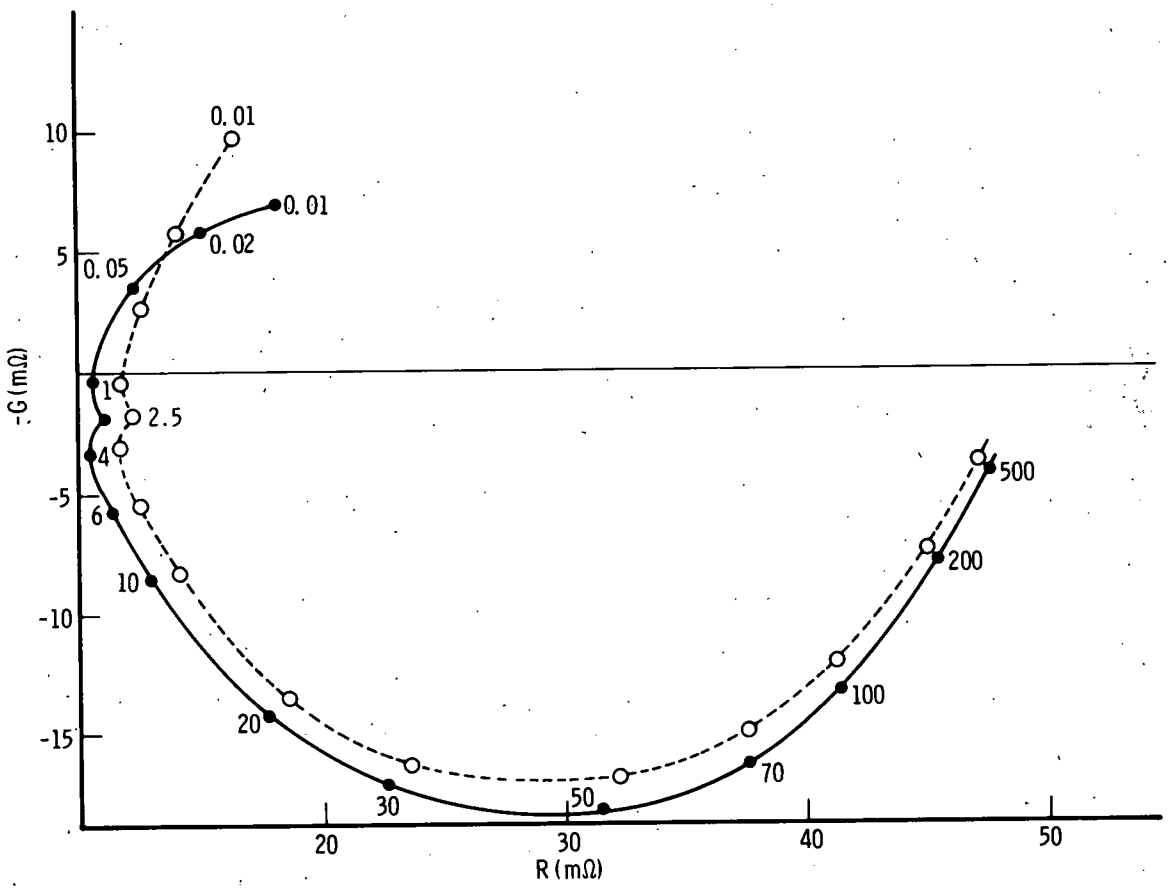

Fig. 2. Impedance of a 2.5 AH Sealed Lead-Acid Gates Cell. The points correspond to the noted frequencies in KHz for the cell 98.5% charged (- - -), and 62.1% charged (——).

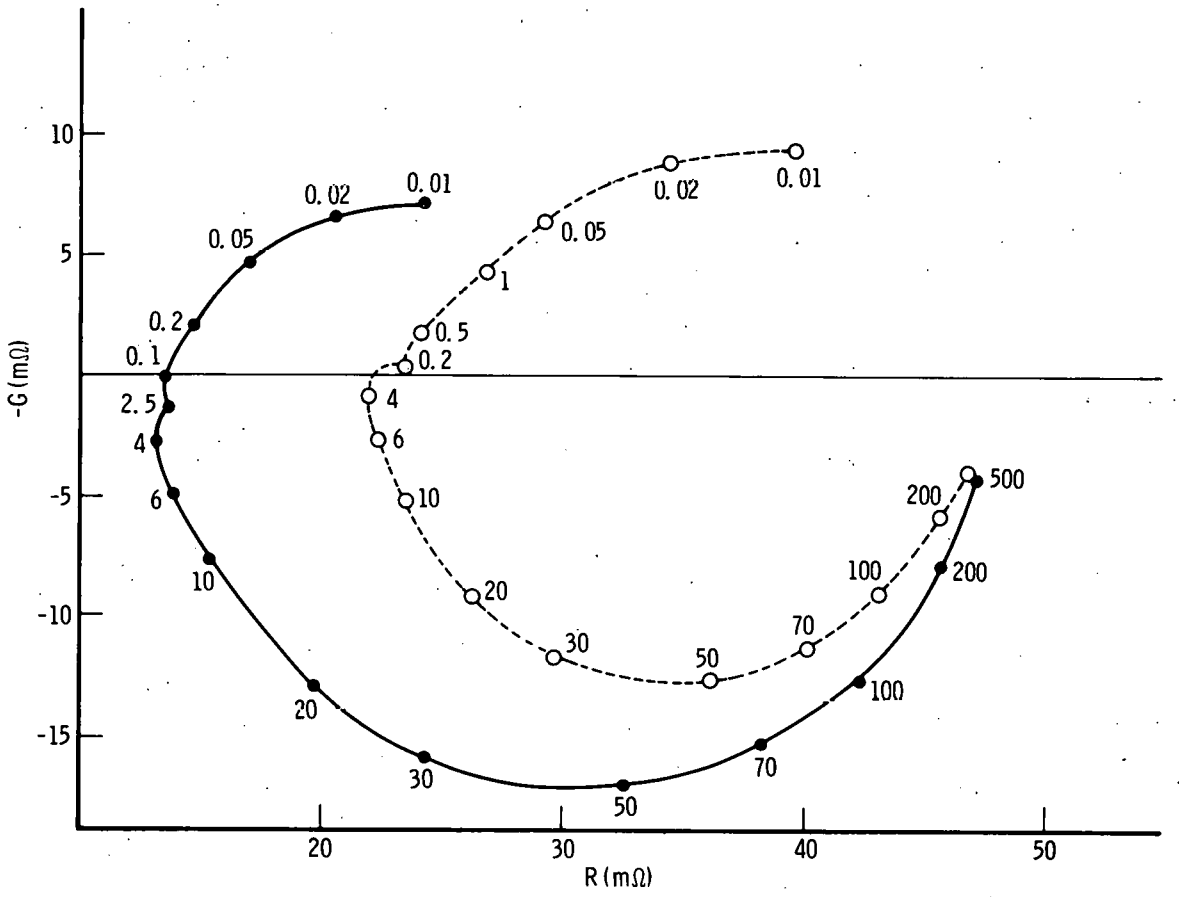

Fig. 3. Impedance of a 2.5 AH Sealed Lead-Acid Gates Cell. The points correspond to the noted frequencies in KHz for the cell 27.9% charged (——) and 12.5% charged (- - -).

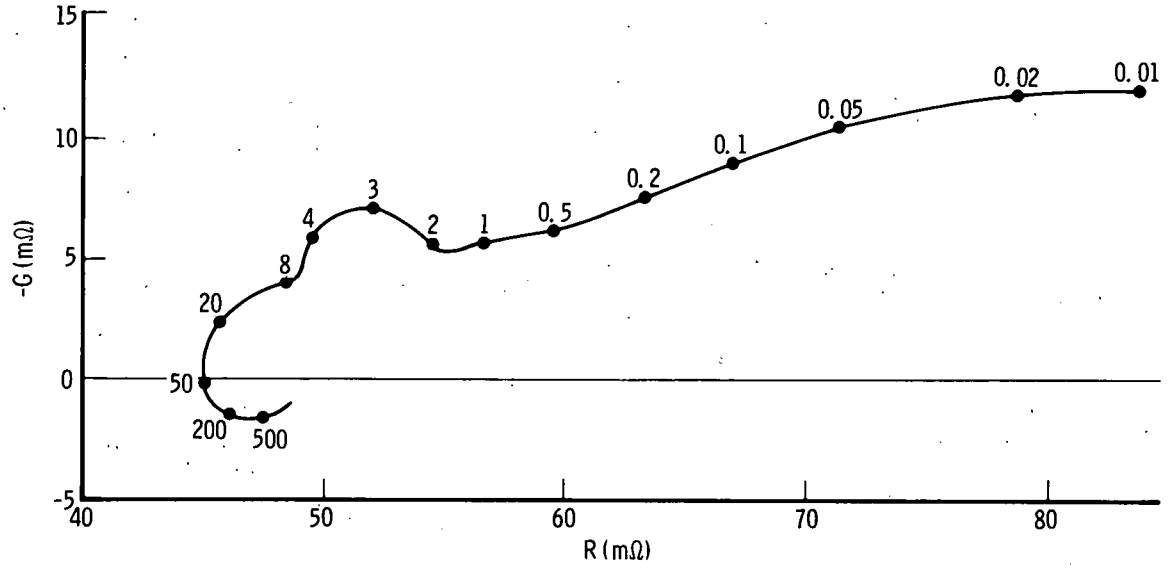

Fig. 4. Impedance of a 3.7% Charged 2.5 AH Sealed Lead-Acid Gates Cell. The points correspond to the noted frequencies in KHz.

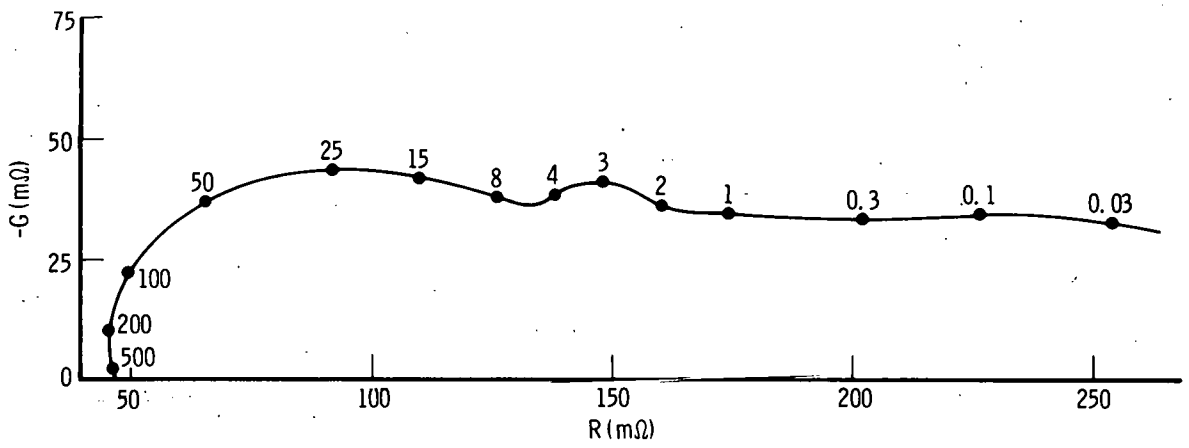

Fig. 5. Impedance of a 2.5 AH Sealed Lead-Acid Gates Cell Completely Discharged (to 1.50 volts at 50 mA). Total discharged capacity was 2.85 AH. The points correspond to the noted frequencies in KHz.

within the cell. When the cell is discharged below about 20% state-of-charge the high frequency inductive arc diminishes in size until at total discharge it is no longer observable (Figures 3 - 5). It is also noteworthy that in all cases the high frequency limit of the cell impedance remains at about 48 mΩ independent of its state of charge.

These observations are consistent with the model of a cell self inductance due to the distributed self inductance of the porous electrodes shunted by the resistance of the electrolyte. This is schematically represented in Figure 6. At high frequencies the impedance represented by Figure 6 will approach a limiting resistance which is significantly greater than the net electrolyte and interfacial resistance. This limiting resistance is expected to be a function of cell geometry and electrode structure and to be essentially independent of cell state of charge. The somewhat distributed nature of the self inductance accounts for the slight distortion of the experimental inductive arcs from the semicircular arcs expected for a pure LR circuit.

At lower frequencies the cell impedance becomes capacitive at all states of charge. At full charge the capacitive impedance is quite pronounced at very low frequencies, while near discharge the capacitive character of the impedance is less pronounced but extends to much higher frequencies. The resistive component of the low frequency impedance consistently increases as the cell is discharged, a result which is a principal cause of the previously noted variation of the phase angle with state of charge.[4] It seems likely that the capacitive impedance at the lowest frequencies results largely from concentration polarization and therefore

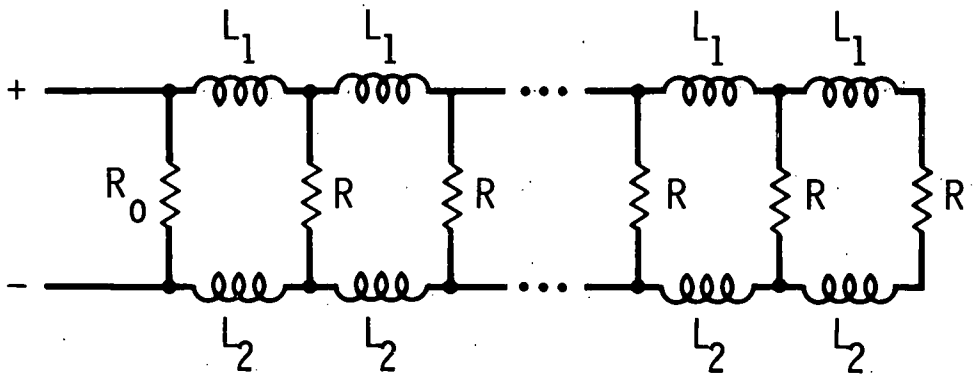

Fig. 6. Cell Self-Inductance Caused by Porous Electrodes

depends on diffusional and transport properties within the cell. This is supported by the work of Keddam et. al.[3] who showed that the impedance of fully charged Pb/H_2SO_4 negative plates at very low frequencies (<1 Hz) behaved like that arising from a Nernst's diffusion layer of finite thickness. In the case of sealed Pb/H_2SO_4 cells mass transport properties are expected to be particularly important as the discharged state is approached since the cells are operating in an electrolyte starved condition.

At frequencies of 1 to 10 KHz a small inductive arc followed by a small capacitive arc is observed in the impedance of charged cells (Figs. 2 - 3). This inductive arc is again likely to be associated with the cell self inductance. The small capacitive arc is seen superimposed on the impedance at about the same frequency for all states of charge, however it becomes significantly more prominent when the cell approaches the discharged state. Near the discharged state a second capacitive arc appears at high frequencies. For the totally discharged state shown in Figure 5 these capacitive arcs may schematically be represented by resistances of about 0.02Ω and 0.09Ω and parallel capacitances of about 4×10^{-3}F and 7×10^{-5}F respectively for the low and high frequency arcs. The former capacitive feature does not change frequency but does grow in size with discharge, indicating that as the resistance in this parallel RC configuration increases, the capacitance decreases correspondingly. This feature could be due to the capacitance of the porous, polarized interfacial layer of $PbSO_4$. The latter capacitive arc which is observed near discharge at very high frequencies is most likely due to the double layer capacity of the Pb grids on which the active material is supported.

The impedance arising from this double layer capacity is observed near discharge where the active materials are nearly depleted, leaving only the lead grids covered with $PbSO_4$.

B. Flat Electrode Pb/H_2SO_4 Wet Cell.

The impedance of a Pb/H_2SO_4 wet cell having flat plate electrodes is presented as a function of frequency in figures 7 and 8 for cell potentials ranging from 2.10 - 1.50 volts. At frequencies greater than about 30 KHz this cell exhibits a self inductive impedance which is essentially independent of cell potential. This is to be expected since this cell has flat rather than highly porous electrodes. The self inductance may schematically be represented by a 1.6×10^{-6} H inductor shunted by a parallel 0.6Ω resistor.

At cell potentials of 2.05 - 2.10 volts the impedance exhibits a gradual capacitive rise at intermediate frequencies, followed by a sharply capacitive rise at the lowest frequencies. As the cell potential decreases below 2.00 volts a capacitive impedance arc characteristic of a double layer capacitance shunted by a parallel charge transfer resistance begins to appear at high frequencies. With decreasing cell potential the charge transfer resistance increases dramatically while the double layer capacity gradually decreases. The result is that the capacitive arc becomes larger and is shifted to lower frequencies as the cell potential decreases. These capacitances and resistances are summarized in Table 1. It is interesting but not entirely unexpected that the charge transfer resistance increases so dramatically near discharge, since this increased resistance is certainly one factor limiting the current from a battery cell as the discharged state is approached.

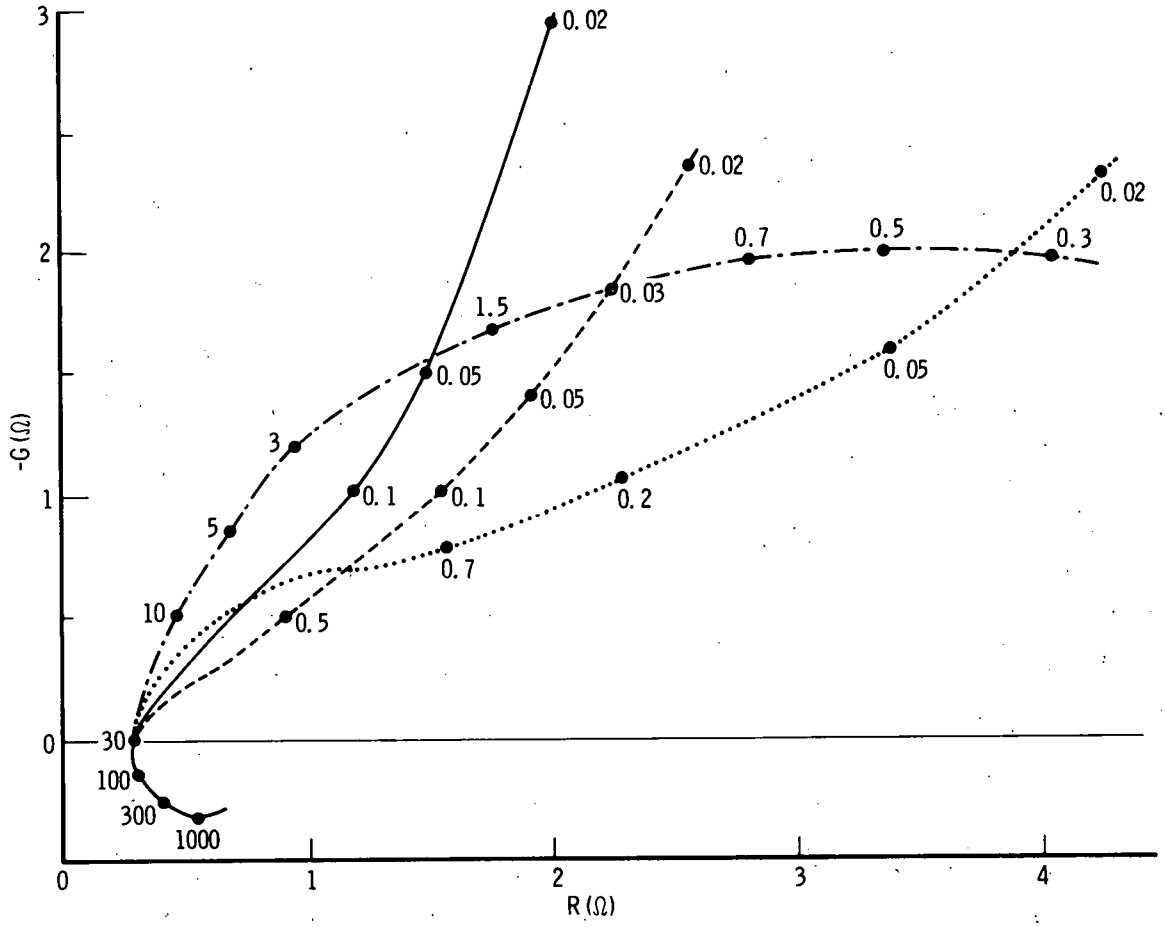

Fig. 7. Impedance of Flat Electrode Lead-Acid Cell at Various Potentials; (——) 2.15 Volts, (- - -) 2.05 Volts, (- - - - -) 2.00 Volts, and (—·—·) 1.95 Volts. The points correspond to the frequencies noted in KHz.

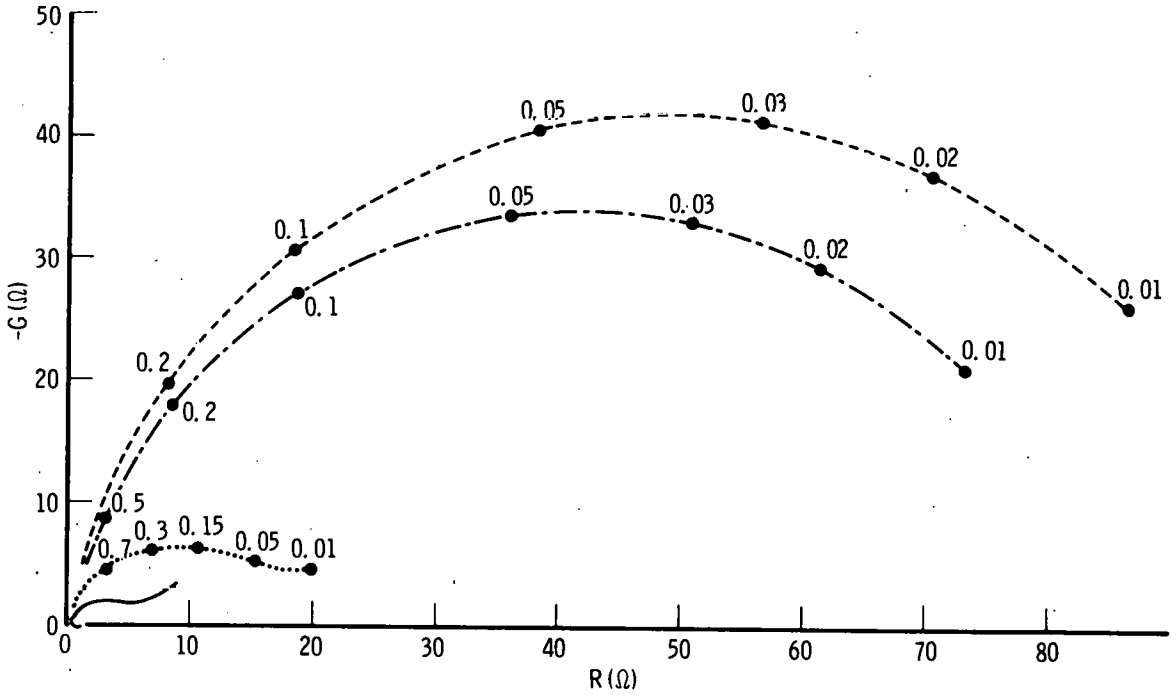

Fig. 8. Impedance of the Flat Electrode Lead-Acid Cell at Various Potentials; (——) 1.95 Volts, (- - - -) 1.90 Volts, (—·—·) 1.80 Volts, and (----) 1.50 Volts. The points correspond to the frequencies noted in KHz.

TABLE 1. Double Layer Capacities and Charge Transfer Resistances Observed for the Pb/H_2SO_4 Wet Cell

Cell Potential (volts)	Capacitance ($\mu F/cm^2$)	Resistance (Ω)
2.00	3.4	1.4
1.95	3.1	4.0
1.90	2.8	12.5
1.80	2.8	68
1.50	2.6	84

For a commercial wet cell Pb/H_2SO_4 battery the recent work by Keddam et. al.[3] has shown that the high frequency capacitive arc arises entirely from the impedance of the negative electrode at full charge. This suggests that the double layer capacities and transfer resistances presented in Table 1 arise from the negative electrode. Furthermore, Tiedemann and Newman[8] have shown that the double layer "capacity" of the positive plate is several orders of magnitude greater than that of the negative. This indicates that the sharply capacitive rise which is observed in the impedance at very low frequencies, particularly at the higher cell potentials, is likely to arise from the positive electrode.

Conclusions

The impedances of both commercial sealed Pb/H_2SO_4 and flat electrode Pb/H_2SO_4 cells have been measured at various states of charge. An overall comparison of these two systems reveal impedance differences due both to differing electrode construction as well as to differing resistances and capacitances. However similarities in overall impedance changes with state of charge are observed which allow comparisons to be made between the two systems.

The changes which were observed in the inductive behavior of sealed Pb/H_2SO_4 cells with discharge indicate that impedance measurements have significant potential for characterizing changes in electrode structure and surface morphology with charge or discharge. These measurements are advantageous over other methods for investigating electrode structure since disassembly of the cells is not necessary.

On the basis of this study the correlation of the phase angle with cell state of charge which is observed at frequencies less than 100 Hz cannot be

explicitly related to electrode changes. In fact the data for the flat elcctrode cell indicate the low frequency phase angle variation ceases to become monotomic as the discharged state is approached. Changes in the phase angle may thus reflect a number of varying electrode, interfacial, or diffusional properties. Detailed impedance measurements at much lower frequencies must be made for the individual cell electrodes before the relationships between low frequency phase angle changes and variations in Pb/H_2SO_4 cell properties can be fully characterized.

References

1. R. J. Brodd and H. J. DeWane, J. Electrochem. Soc., 110 (1963) 1091.
2. M. Lurie, H. N. Seiger, and R. C. Shair, Gulton Industries Technical Documentary Report ASD-TDR-63-191, 1963.
3. M. Keddam, Z. Stoynov, and H. Takenouti, J. Applied Electrochem., 7 (1977) 539.
4. M. R. Martinelli and C. C. Badcock, unpublished work.
5. E. Willihnganz, J. Electrochem. Soc., 102 (1955) 99.
6. J. J. Lamden and E. E. Nelson, ibid. 107 (1960) 723.
7. F. Gutman, ibid. 112 (1965) 94.
8. W. Tiedemann and J. Newman, ibid. 122 (1975) 70.

DISTRIBUTION

Internal

C. Badcock
S. Birken
S. Feuerstein
L. Gibson
F. G. Gorman
W. Graham
H. Heritage
J. Kettler
H. Killian
G. W. King
W. Leverton
M. R. Martinelli
S. Mayer
R. X. Meyer
J. Nicklas
V. Profumo
P. Sheldon
S. Siegel
D. Slocum
W. Stafford
E. T. Welmers
A. H. Zimmerman

External

SAMSO (YCPT)
Lt. A. G. Fernandez

Scientific and Tech. Info. Facility
P. O. Box 33
College Park, Md. 20740
Attn: NASA Rep.

Science and Technology Division
Director of Development
DCS/R&D
Washington, D.C. 20330

ESD (TRI)
Hanscom AFB, Mass. 01731

AFSC (DLF)
Andrews AFB, D.C. 20331

AFML (NA)
Wright-Patterson AFB, Ohio 45433

AFFDL (SU)
Wright-Patterson AFB, Ohio 45433

AFRPL (XP)
Edwards AFB, Calif. 93523

AFAL (CA)
Wright-Patterson AFB, Ohio 45433

SEG (SEPI)
Wright-Patterson AFB, Ohio 45433

AFAPL (NA)
Wright-Patterson AFB, Ohio 45433

AFWL (SUL)
Kirtland AFB, New Mex. 87117

RADC (XP)
Griffiss AFB, New York 13442

AFGL (XOP)
Hanscom AFB, Mass. 01731

AEDC (ER)
(Library)
Arnold AFB, Tenn. 37389

AFOSR (NC)
Bolling AFB, D.C. 20332

Air University Library
Maxwell AFB, Ala. 36112

AFIT (Tech Library)
Wright-Patterson AFB, Ohio 45433

FJSRL (NA)
USAF Academy, Colo. 80840

Library
U.S. Dept. of Commerce
Environmental Sciences Services Admin.
Boulder Labs
Boulder, Colo. 80302

NASA (Library)
Lewis Research Center
21000 Brookpark Road
Cleveland, Ohio 44135

NASA (Library)
Marshall Space Flight Center
Huntsville, Ala.

National Bureau of Standards
(Library)
Washington, D.C. 20234

Naval Ordnance Lab (Tech Library)
White Oaks
Silver Springs, Md 20919

U.S. Army Signal Res. and Dev't. Lab
Data Equipment Branch
Technical Information Officer
Fort Monmouth, N.J. 07703

ONR Branch
Commanding Officer
1030 Green Street East
Pasadena, Calif. 91100

NASA (Library)
Ames Research Center
Moffett Fields, Calif. 94035

NASA (Library)
Langley Research Center
Langley Field, Va. 23365

NASA (Library)
Johnson Space Center
Houston, Texas 77058

Jet Propulsion Laboratory
4800 Oak Grove Drive
Pasadena, Calif. 91103

U.S. Atomic Energy Commission
Director of Research
Washington, D.C. 20025

U.S. Atomic Energy Commission
Tech. Info. Service Extension
P.O. Box 62
Oak Ridge, Tenn. 37830

Naval Research Lab (Library)
Washington, D.C. 20025

Commanding Officer
Harry Diamond Laboratories
U.S. Army Materiel Command
Washington, D.C. 20438
Attn: Library